Measured and Simulated Distributions of Voltage and Temperature along Stator Coils of Synchronous Generator

Jan KACEROVSKY, Ondrej KRPAL, Frantisek MACH

Department of Theory of Electrical Engineering, Faculty of Electrical Engineering, University of West Bohemia in Pilsen, Univerzitni 26, 306 14 Pilsen, Czech Republic

jankac@kte.zcu.cz, okrpal@ket.zcu.cz, fmach@kte.zcu.cz

DOI: 10.15598/aeee.v13i4.1401

Abstract. *The ECP (end winding corona protection) of the armature coils of a synchronous generator is designed and modeled. The paper focuses on the distribution of voltage and temperature along this protection that is both measured and simulated. The results are compared. The aim of the work is to verify the suggested mathematical model which would help to save time and costs connected with the ECP design.*

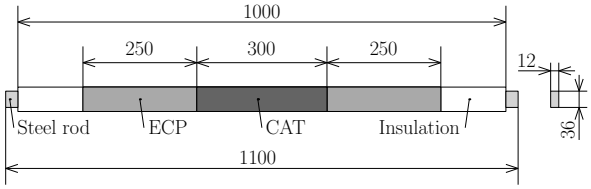

Fig. 1: Illustrative sample and geometry of the end part of winding (dimensions given in mm, CAT denoting the conductive armor tape).

Keywords

End winding corona protection, simulation, surface discharges, synchronous generator, temperature distribution, voltage distribution.

1. Introduction

The ECP is applied to the end part of windings of synchronous generators to reduce the gradient of the local electric field and development of connected undesirable phenomena (surface discharges). An appropriate design of this protection, that is exposed to mechanical, electrical and thermal stresses during the operation of the machine, can prolong the time of its maintenance and overall lifetime. The paper deals with the measurement and simulation of ECP to facilitate its design. The illustrative sample and its geometry of the end part of winding is shown in Fig. 1.

2. Formulation of the Problem

The correct function of the ECP follows from its appropriate selection and method of the ECP application. The ideal ECP should linearize the voltage distribution as much as possible (the field should be constant along the length of the ECP) and the voltage at the end of the protection should not lead to any surface discharges, i.e., its value should be closest to the voltage on the conductor (Fig. 2). In addition, the ECP has to prevent itself from its own overheating, i.e., its ohmic losses must not exceed the prescribed value.

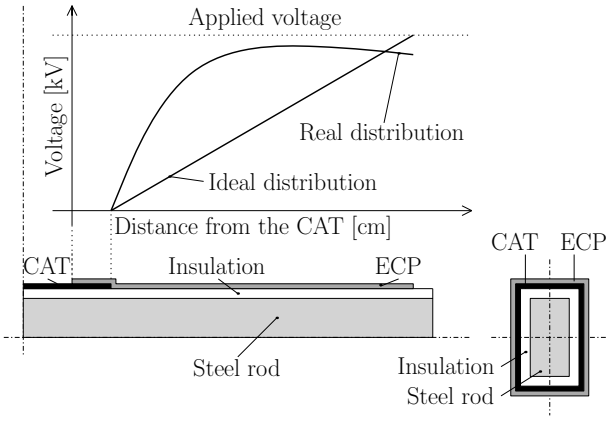

Fig. 2: Real and ideal voltage distribution [1].

3. Mathematical Model

The mathematical model of the voltage distribution along the semiconducting protection (ECP) is described by the Eq. (1):

$$\mathrm{div}((\sigma + j\omega\varepsilon) \cdot \mathrm{grad}\varphi) = 0, \tag{1}$$

where σ denotes the electric conductivity, φ is the electric potential and ε stands for the permittivity. The boundary conditions are given by the known values of the electric potential on the inside edges of the insulation from the direction of the steel rod (45 kV) to the copper tape (0). The Neumann condition $\partial\varphi/\partial n_0 = 0$ is placed on the outside edges of the CAT, ECP and insulation.

The mathematical model of the steady-state heat transfer along the semiconducting protection (ECP) is described by the Eq. (2):

$$\mathrm{div}(\lambda \cdot \mathrm{grad}\ T) + p = 0, \tag{2}$$

where λ is the thermal conductivity, T denotes the temperature and p means the heat losses. The plane of symmetry of the sample is characterized by the Neumann boundary condition ($\partial T/\partial n = 0$), while the walls of the rod are characterized by the mixed boundary condition in the form $-\lambda \cdot \partial T/\partial n_0 = \alpha \cdot (T - T_{\mathrm{ext}})$, where α expresses the convective coefficient, T stands for the surface temperature and T_{ext} is the external temperature.

The losses produced in the ECP can be divided into two main parts: Joule losses and dielectric losses. Their volumetric value p can be determined as $p = p_{\mathrm{j}} + p_{\mathrm{d}}$, where the volumetric Joule losses are given as $p_{\mathrm{j}} = \sigma \cdot E^2$ and the volumetric dielectric losses are expressed as $p_{\mathrm{d}} = \omega \cdot \varepsilon \cdot E^2$.

4. Simulation

The present time offers new possibilities of numerical calculations, especially using the finite element method (FEM). Calculation of the 3D distributions of both electric and temperature fields provides a comprehensive view of the situation in the investigated system.

The computations of voltage and temperature along the rod were realized by the professional code COMSOL® Multiphysics.

The first step was to create the geometry of the sample. For the model, the dimensions $12 \times 36 \times 550$ mm of the steel rod were considered. The thickness of insulating elements is 3.46 mm and the CAT thickness is 0.2 mm. The thickness of the ECP is 0.5 mm. The length of the ECP protection is 250 mm. The ECP protection overlaps the modeled CAT protection by 20 mm. The complete geometrical arrangement of the sample is shown in Fig. 3.

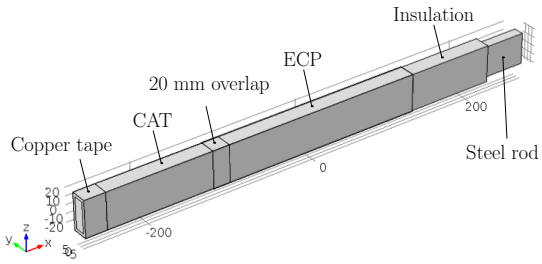

Fig. 3: Geometrical arrangement of the sample for simulation.

The individual parts of the sample are characterized by material parameters summarized in Tab. 1.

Tab. 1: Material parameters of individual parts of the model.

	Insulation	**ECP**
ε_{r} [–]	4	12
σ [S · m^{-1}]	$1 \cdot 10^{-13}$	optional
λ [W · (m · K)$^{-1}$]	0.2	20
	CAT	**Steel rod**
ε_{r} [–]	4	1
σ [S · m^{-1}]	$2.5 \cdot 10^{-3}$	$4.032 \cdot 10^{6}$
λ [W · (m · K)$^{-1}$]	30	44.5

The dependence of electrical conductivity of the ECP on the electric field strength is depicted in Fig. 4.

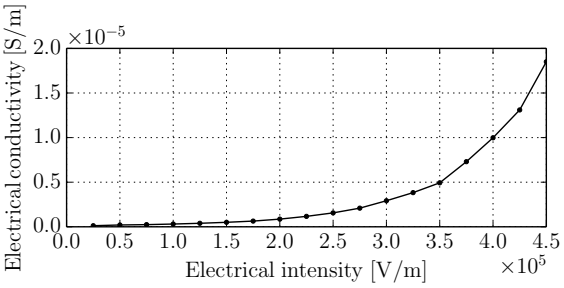

Fig. 4: Electrical conductivity of ECP.

The value of the applied voltage on the steel rod is 45 kV, its frequency being 50 Hz. The heat transfer coefficient is $\alpha = 5$ W/(m^2 · K), the initial temperature of the sample is $T = 293.15$ K and the external temperature is $T_{\mathrm{ext}} = 293.15$ K.

The 3D geometrical arrangements of the sample together with the simulated voltage and temperature distributions are shown in Fig. 5 and Fig. 6, respectively.

The average specific Joule losses and specific dielectric losses in the ECP are compared in Tab. 2. The significance of the dielectric losses is almost negligible.

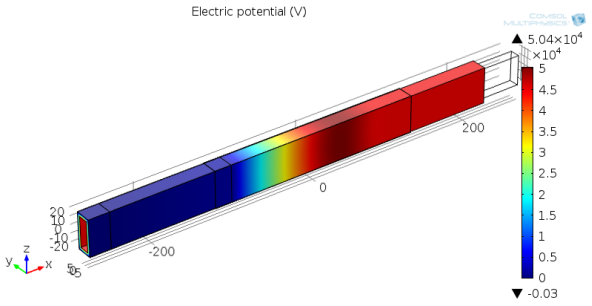

Fig. 5: Simulated 3D voltage distribution along the end part of winding.

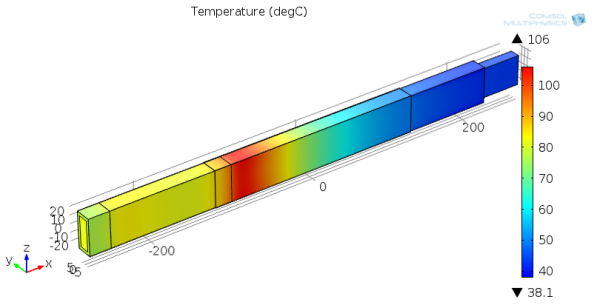

Fig. 6: Simulated 3D temperature distribution along the end part of winding.

Tab. 2: Comparison of the average specific Joule and specific dielectric losses.

Joule losses [W·m^{-3}]	Dielectric losses [W·m^{-3}]
$1.59637 \cdot 10^6$	4082

5. Experiment and Results

The sample was overlapped by the ECP of type A (strong stress-grading characteristic) in the length of 250 mm. For the measurement of the voltage distribution, the voltage was connected to the steel rod. The applied voltage for a comparison of the measured and simulated distributions of voltage and temperature was 45 kV. The CAT was connected to the ground in order to obtain a grounded magnetic circuit. The measuring voltage electrode was gradually shifted by one centimeter from the beginning of the ECP to its end. The voltage distribution was measured along the ECP surface according to Fig. 7.

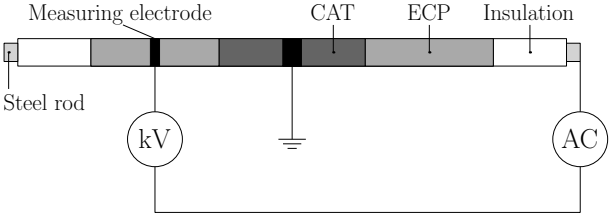

Fig. 7: Arrangement of measurement of voltage distribution.

Figure 8 illustrates the measured voltage distributions for different voltage levels on the semiconducting protection (ECP).

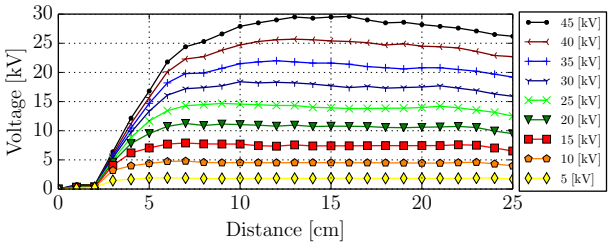

Fig. 8: Voltage levels on the semiconducting protection.

The temperature distribution was measured by a thermocamera in the shot area according to Fig. 9. The voltage was also connected to the steel rod and the CAT was connected to the ground.

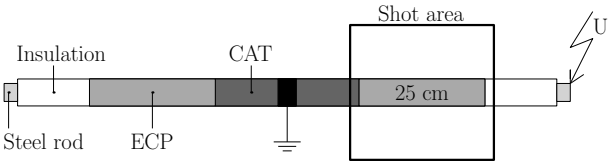

Fig. 9: Arrangement of measurement of temperature distribution.

Figure 10 shows the temperature distribution measured by the thermocamera for voltage 45 kV applied to the conductor. The thermocamera allows exporting data from the shot. In the figure, a straight line is depicted, along which the graph is captured. This graph is then used for comparing the measurement with simulation.

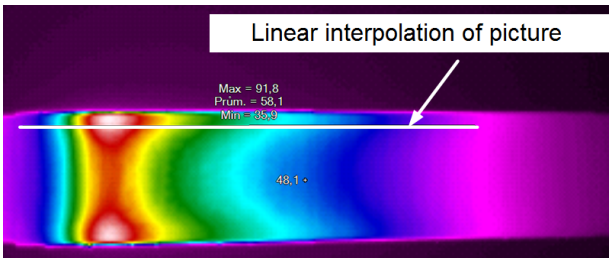

Fig. 10: Picture of end part of winding made by FLUKE thermocamera.

Figure 11 and Fig. 12 show the comparison of the measurement and simulation for voltage 45 kV applied to the conductor.

6. Conclusion

The graph of voltage distribution (see Fig. 11) shows that about 7 cm from the beginning the ECP voltage starts varying. This phenomenon may be due to an increase of influence of the impedance measuring device

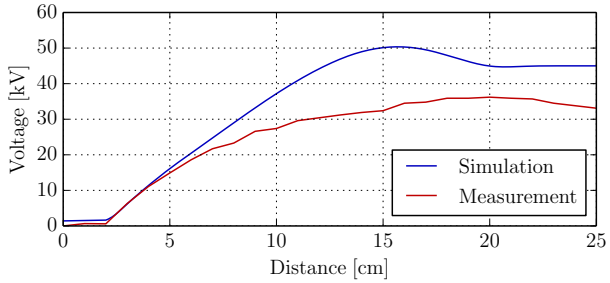

Fig. 11: Picture of end part of winding made by FLUKE thermocamera.

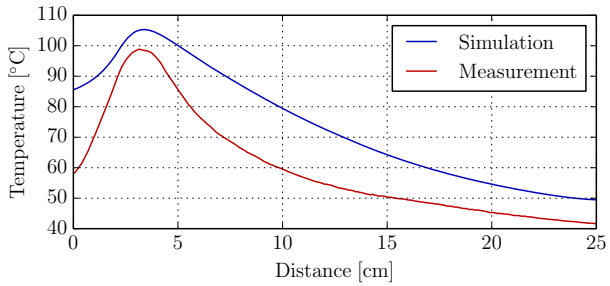

Fig. 12: Picture of end part of winding made by FLUKE thermocamera.

on higher voltages [2]. This could cause a reduction of nonlinearity and electrical conduction of the ECP tape, which results in the dependence of resistivity on the gradient of the applied electric field. Another cause of the voltage drop may consist in the capacitance current passing through the protection at the end of the ECP, whose effect is the phase shift between the voltage and current, i.e., the Ferranti effect. The difference in the above voltage distributions brings the difference between the measured and simulated data for temperature distribution (see Fig. 12). Nevertheless that the results have quite high difference between measurement and simulation, the difference is acceptable for real applications, because when the stator coils are designed by the simulation, the coils will be designed excessively in comparison with designing by the measurement.

Acknowledgment

This paper was supported by an project SGS-2012-39: Advanced methods of theoretical and applied research in electrical engineering and project SGS-2012-026: Material and technological systems in electrical engineering.

References

[1] ROBERTS, A. Stress Grading for High Voltage Motor and Generator Coils. *IEEE Electrical Insulation Magazine*. 1995, vol. 11, no. 4, pp. 26–31. ISSN 0883-7554. DOI: 10.1109/57.400761.

[2] SCHMERLING, R., F. JENAU, S. KEMPEN and F. POHLMANN. Evaluation and Comparison of Measurement Methods for Determining the Electrical Potential at Surfaces by Using the Example of End Corona Protection Configuration. In: *17th International Symposium of High Voltage Engineering*. Hannover: Leibniz Universitat, 2011, pp. 1347–1351. ISBN 978-3-8007-3364-4.

[3] MALAMUD, R. and I. CHEREMISOV. Mechanism of Funcionality of Semiconductive Materials and Reliable Anti-Corona Protection Designs of High-Voltage Generator Windings. In: *Conference on Electrical Insulation and Dielectric Phenomena (CEIDP 2007)*. Vancouver: IEEE, 2007, pp. 580–583. ISBN 978-1-4244-1482-6. DOI: 10.1109/CEIDP.2007.4451569.

[4] CHRISTEN, T., L. DONZEL and F. GREUTER. Nonlinear resistive electric field grading part 1: Theory and simulation. *IEEE Electrical Insulation Magazine*. 2010, vol. 26, iss. 6, pp. 47–59. ISSN 0883-7554. DOI: 10.1109/mei.2010.5599979.

[5] ALLISON, J. A. Understanding the need for Anti-corona materials in High Voltage Rotating machines. In: *Proceedings of the 6th International Conference on Properties and Applications of Dielectric Materials*. Xi'an: IEEE, 2000, pp. 860–863. ISBN 0-7803-5459-1. DOI: 10.1109/ICPADM.2000.876364.

[6] MALAMUD, R. and I. CHEREMISOV. Anti-corona Protection of the High Voltage Stator Windings and Semi-Conductive Materials for Its Realization. In: *IEEE International Symposium on Electrical Insulation*. Anaheim: IEEE, 2000, pp. 32–35. ISBN 0-7803-5931-3. DOI: 10.1109/ELINSL.2000.845414.

[7] OMRANIPOUR, R. and S. U. HAQ. Evaluation of Grading System of Large Motors AC Stator Winding. In: *IEEE International Symposium on Electrical Insulation*. Vancouver: IEEE, 2008, pp. 158–161. ISBN 978-1-4244-2091-9. DOI: 10.1109/ELINSL.2008.4570300.

About Authors

Jan KACEROVSKY graduated from the Faculty of Electrical Engineering, University of West Bohemia in

Pilsen, in 2012. He is currently Ph.D. student at the same university and he is interested in electrostatic separation of mixture of plastic particles. He is an author or coauthor about 10 refereed papers.

Ondrej KRPAL graduated from the Faculty of Electrical Engineering, University of West Bohemia in Pilsen, in 2010 and finished his postdoctoral studies in 2014. He is interested in optimization of ECP protections along stator bar. He is an author or coauthor about 20 refereed papers. He also worked for 5 months as a trainee in Maschienenfabrik Reinhausen (Regensburg, Germany).

Frantisek MACH graduated from the Faculty of Electrical Engineering, University of West Bohemia in Pilsen, in 2011. He is currently Ph.D. student at the same university. His research interests include computational electromagnetics, coupled problems. He is an author or coauthor about 40 refereed papers, and he is also Agros2D contributor.